3D printing of multifunctional polymer for space application

Ugo Lafont*, Bruno Delacourt*, Maria Terol-Sanchez**, Mathis Munck*, Johanna Wessing*
and Riccardo Rampini*
* European Space Agency
Keplerlaan 1, PO Box 299, 2200 AG Noordwijk, The Netherlands
**Material Science and Engineering, Delft University of Technology
Mekelweg 2, 2628 CD Delft, The Netherlands

Abstract

The European Space Agency is looking into the implementation and use of new materials to enable new applications for space from ground to out-of-earth application in combination with 3D printing process. In this respect, development of electrically conductive high performance thermoplastic like PolyEtherEtherKetone (PEEK) has been achieved using carbon nanotubes and graphene as fillers, enabling new applications aiming at metallic part replacement. In view of future space application, the effect of space environment (VUV, Thermal Cycling, ATOX) on the functional performance of the material have been assessed. The results obtained on this material mechanical, optical and electrical (ESD, electrical conduction and data transfer capabilities) performances are presented. Test performed on a PEEK based electrically conductive 3D printed payload for a CubeSat are detailed in this paper.

1. Introduction

Within the thermoplastic family, so called high performance and engineering thermoplastics have a great potential for applications where structural, resistance to wide thermal range, chemical stability are driving requirements. They have found their way for high demanding application in the aerospace, automotive and energy sector among other, allowing replacement of metallic based parts, producing lighter structure, allowing mass production and reducing the processing energy needs. The advantage of thermoplastics, beside their interesting intrinsic properties, lies in their processing: due to the presence of a melting point, they can be melt processed, combined with fillers to create new functionalities, welded, recycled, and do not suffer of shelf life issues like thermoset prior curing. Among the available choice of high performance materials that will meet the most demanding applications including space the following can be listed: Polyetherimide (PEI) / Polysulfone (PSU) / Polyethersulfone (PES) Polyphenylsulfone (PPSU), Polyetheretherketone (PEEK) / Polyetherketoneketone (PEKK) / Polyphenylene sulfide (PPS) / Polytetrafluoroethylene (PTFE) / Polyvinylidene fluoride (PVDF) / Fluorinated ethylenepropylene (FEP). Some other candidates classified as engineering thermoplastics in opposition to commodity thermoplastics and used in earth based application could be fit for space applications depending on the requirements and the functional environment: Polycarbonate (PC) / Polyphenylene oxide (PPO) / Polyphenylene ether (PPE) Thermoplastic Urethane (TPU), Polyoxymethylene (POM) / Polyethylene terephthalate (PET) / Polyamide (PA6 / PA11 / PA12). Combining additive manufacturing with its advantage in term of new design capabilities including topological optimization and on demand manufacturing opportunities together with high performance thermoplastics is a clear asset to further reduce the weight of certain parts, decrease manufacturing time and cost, keeping a high level of functionality and enable new functionalities or applications.

Using thermoplastics to replace metallic parts in space application is under evaluation within the HighPEEK ESA (European Space Agency) financed project [1]–[3]. This approach focus on productivity and mass gain as well as development and implementation of electrically conductive high performance thermoplastics. For this purpose, several demonstrators (Fig. 1) have been produced via Fused Filament Fabrication (FFF) process (3D printing) using first high performance thermoplastics (CF-PEEK) and later modified high performance thermoplastics with electrical conduction capabilities (electrically conductive PEEK). Structural elements, electronic box enclosures (power relay, on-board computer and sensor housing) were tested toward space qualification including electrical conduction, space environment (outgassing, thermal cycling and UV exposure), mechanical performance evaluation and vibration test. The first output of this activity demonstrate that ~60% in mass reduction can be achieved compare to Aluminium baseline due to the implementation of new design concept enable by the manufacturing process.

Lafont, Delacourt, Terol-Sanchez, Munck, Wessing and Rampini

Figure 1: (Left) Re-designed IRES-C sensor housing printed using CF-PEEK and (Right) thermoplastic composite corner bracket. (Image credit: MiniFactory Oy LTD [2])

New material development is also a key aspect in relation to space application. Thermoplastics with enhance functionalities (thermal, electrical, self-healing) will further increase filed of application. Electrically conductive PEEK was developed incorporating Carbon Nanotubes (CNTs) and Graphene Nano Platelets (GNPs) into PEEK [4]. The resulting nano-composite material exhibit an intrinsic direct current electrical conductivity of 13 $S.m^{-1}$, enhanced thermal conductivity and 60% reduction in coefficient of friction. This material in form of a 1.75 mm diameter filament will be used in this study (Fig. 2).

Finally, combination of different materials during the FFF process (multi-material printing) is providing to engineers new capabilities in term of design and applications. With thermoplastics, multi-material printing is relying on 3D printers equipped at least with dual extrusion capabilities. Even if such printers are widely available commercially, very few of them are able to process at the same time high performance thermoplastics like PEEK that requires, high extrusion temperature and enclosed chamber with high temperature. Combining PEEK and electrically conductive PEEK has been achieved with dual-printing (Fig. 2). Such combination allows to create conduction path directly embedded into a part. From cube-sat bodies [5] to electrical component [6] applications are emerging. For the last case, the capabilities offered by such material combination forming an electrical circuit fully made of polymers has been tested for data transmission: a transfer rate of 115200 bits per second was achieved using electrically conductive PEEK [7].
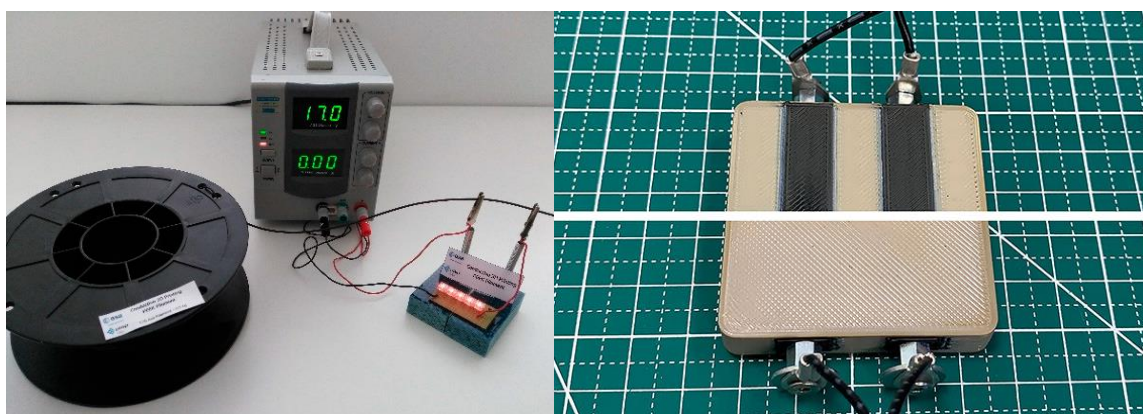

Figure 2: (Left) Electrically conductive PEEK filament developed and used in this study and (Right) Parts produced using dual-printing with PEEK and conductive PEEK (in black) with embedded conductive path used for testing data transfer capabilities [7] (Image credit: Zortrax/ESA/PIEP)

In order to accelerate the implementation of this material for space application, there is a need to have a clear vison of the advantages and limitations. The advantage of thermoplastics with multifunctional properties and additive manufacturing focusing on Fused Filament Fabrication (FFF) process are discussed specially looking at the material process relationship and the effect of space environment on electrically conductive PEEK based parts: effect of thermal vacuum cycling and vacuum UV exposure on the mechanical and thermo-optical performance, effect of atomic oxygen,

and suitability toward electrostatic discharge. Finally, test performed on a flight demonstrator, designed to act as an electrical circuit to be implemented as payload into a cubesat are presented.

2. Materials and methods

Electrically conductive PEEK-based filament suitable for 3D printing process and used in this study was developed by PIEP incorporating of 4 wt.% of multi-walled carbon nanotubes supplied by Nanocyl and 3 wt.% of graphite nano-platelets supplied by XG Science Inc into Victrex 450G PEEK [4]. The standard non-conductive PEEK filament used was Z-PEEK from Zortrax.

The 3D printing of the conductive PEEK based samples used in this study for the assessment of the effect of space environment was achieved using an APIUM P220 3D printer from 2018. For dual printing purpose (PEEK and Conductive PEEK), the Endureal 3D printer from Zortrax from 2020 was used.

The 3D printed demonstrator for CubeSat consists in two pads of conductive PEEK printed together within a non-conductive PEEK block using dual printing process. In each of the two pads, two gold platted metallic pins have been inserted in order to connect the electrical path to a PCB that include a LED (light-emitting diode) facing a LDR (light-dependent resistor). The equivalent electrical circuit diagram in illustrated in Figure 9.

Flexural properties assessment was performed following the ASTM D790 standard using a three-point bending test fixture on a Zwick/Roell Z100 equipped with a 2.5 kN load cell using a support span of 64 mm. The test were performed at a strain rate of 1.7 mm.min^{-1} and applying a pre-load of 10 N. Samples for flexural test were produced based on the ASTM D790 geometry (rectangular shape 80 x10 x 4 mm). Several samples were 3D printed using only PEEK, conductive PEEK or bi-material PEEK/Conductive PEEK. The composite samples PEEK/Conductive PEEK present in its thickness 2 mm of PEEK and 2 mm of conductive PEEK. For each configuration 5 samples were printed and tested (N=5).

Material outgassing evaluation was done following the ECSS-Q-ST-70-02C standard at ESA/ESTEC premise [8].

Thermal vacuum cycling was performed in a specific chamber for 20 cycles from -100 °C to +100 °C with a vacuum level between 10^{-6} and 10^{-7} mbar using a 4 K/min heating rate.

The UV/Vacuum UV (VUV) radiation testing was carried out in the CROSS1 facility at ESA/ESTEC premise (Fig. 3). The facility consists of a high vacuum chamber operated at 10^{-5} mbar, a sample plate assembly and a cold shroud cooled by liquid nitrogen. The UV irradiation set-up consists of an array of 4 halogen discharge lamps in open quartz (PhilipsHPA-690 400 W Halogen) which produces UV, visible and IR radiation positioned outside the vacuum chamber and illuminating the sample plate at normal incidence. The VUV (vacuum UV) lamps are L2D2 deuterium lamps (L7293series from Hamamatsu) radiating the sample plate under 45 angle. The irradiation was done for 140.6 hours. During the test the samples temperature reached 170 °C. The used irradiative condition correspond to 3.4 solar constant resulting in 478.4 equivalent sun hours. After the UV/VUV exposure cycle, a set of sample were taken out from the chamber for measurement purpose whereas another set of samples was left into the CROSS1 chamber and was subjected to subsequent 6 thermal vacuum cycling between -100 °C and +100 °C at 10^{-5} mbar.

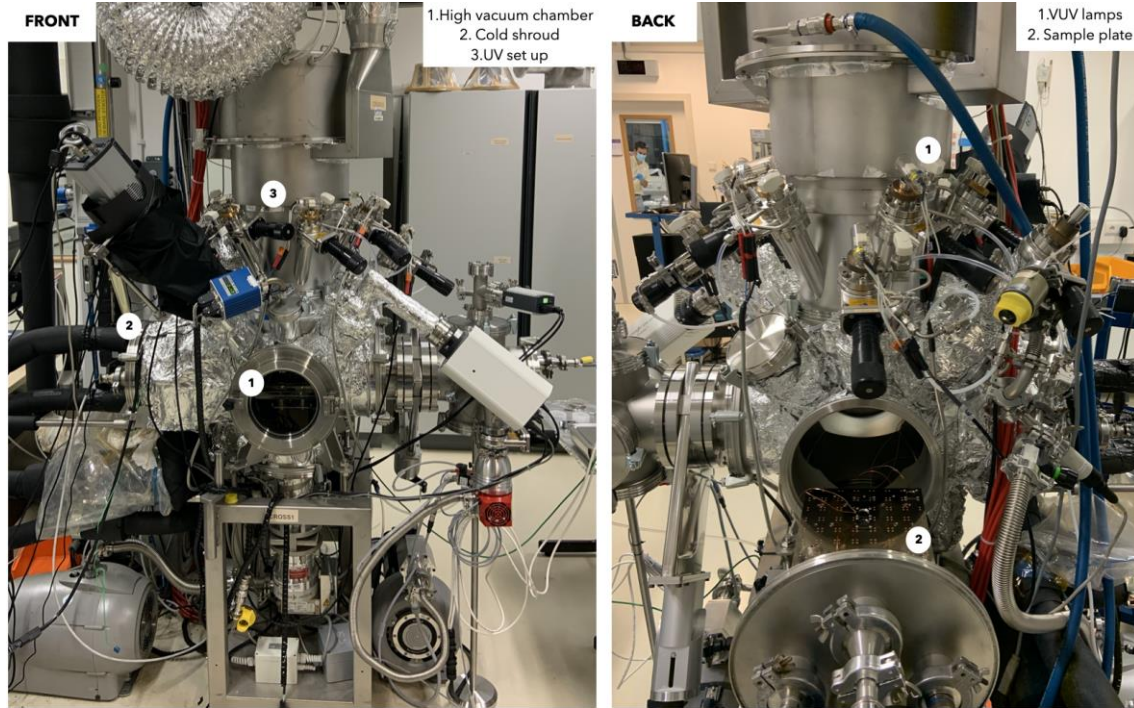Lafont, Delacourt, Terol-Sanchez, Munck, Wessing and Rampini

Figure 3: CROSS1 facility at ESA/ESTEC used for UV and Vacuum UV exposure

Atomic Oxygen exposure (ATOX) was performed in ESTEC TEC-QEE Laboratory LEOX facility at ESA/ESTEC premises. Atomic oxygen produced by dissociation of molecular O_2 using pulsed CO_2 laser. The fluxes generated are around 1×10^{20} atoms/cm² per day with a typical atomic oxygen energy of 5.5 eV. The erosion yield is calculated using Equation 1.

$$E = \frac{\frac{(M_{BOT} - M_{EOT})}{1000}}{A_s \rho_s F} \tag{1}$$

Where, M_{BOT} is the mass of sample before the test (mg), M_{EOT} the mass of sample at the end of test (mg), A_s the exposure area (3.14 cm^2), ρ_s the sample density (g/cm^3) and F the atomic oxygen fluence (atoms/cm^2).

Electrical charging behaviour was assessed in the ESD facility [9] at ESA/ESTEC premise. Its test chamber operate below 10^{-6} mbar. Samples or test assemblies lie on a grounded baseplate that can be temperature-controlled down to -240 °C using a compressed helium cooling system. Surrounding the baseplate, a grounded cryogenic shroud can be cooled to -150 °C using liquid nitrogen circulation. When cold, the shroud limits thermal radiations. Also it is cooled down before the baseplate to allow remaining gas to condense on its surface and protect the test specimen. The ESD facility enables exposure of samples and assemblies to mono-energetic electrons from 5 to 60 keV and/or to vacuum UV (110 to 200 nm). The electron gun (Staib Instrumente EK-6000-E1) provides a homogenous beam over the entire test specimens. The usable electron flux ranges from 0.1 to 10 nA·cm^{-2}. It is measured via a Faraday cup placed in the vicinity of the sample and connected to an ammeter.

BOF facility at ESA/ESTEC premises was used to test the 3D printed payload demonstrators for CubeSat qualification models (QM) in order to perform functional test in vacuum and at representative operating temperatures (Figure 4).
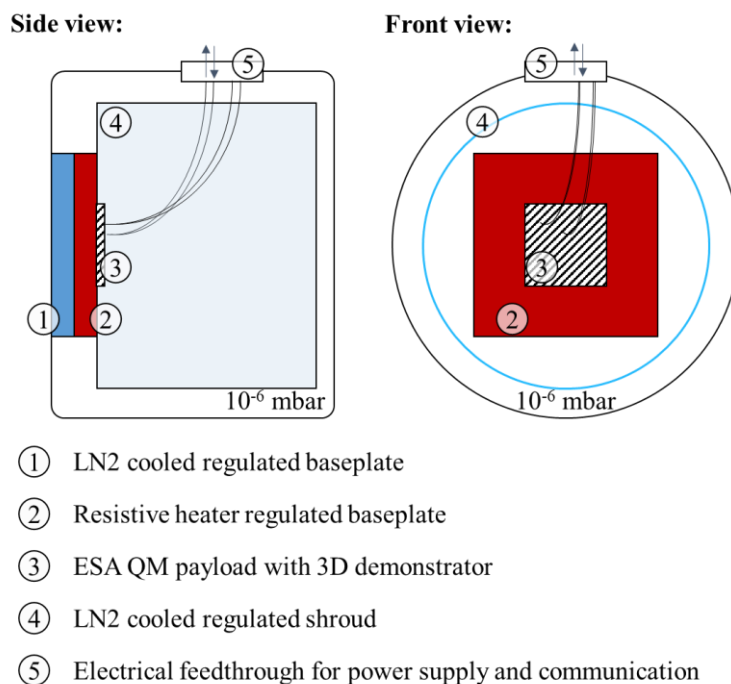
① LN2 cooled regulated baseplate

② Resistive heater regulated baseplate

③ ESA QM payload with 3D demonstrator

④ LN2 cooled regulated shroud

⑤ Electrical feedthrough for power supply and communication

Figure 4: Simplified schematic of BOF facility used to perform the functional test in vacuum ($< 10^{-6}$ mbar) at mission's representative operating temperatures.

An Agilent Cary 5000A UV/VIS/NIR spectrophotometer fitted with an internal integrating sphere was used to acquire the total reflectance of the samples between 2500 and 250 nm under ambient conditions. Reflectance measurements were corrected against a calibrated specular standard (02% diffuse working standard). For the determination of the Solar absorptance (α), total reflectance spectra were weighted against the Sun spectrum. The uncertainty of the solar absorptance determination through this method is ±0.03 (confidence factor = 2).

Thermal emittance (ε) was measured using a TESA 2000B portable reflectometer/emissometer from AZ technology. The IR emittance is obtained by integrating over the spectral range from 3 μm to 30 μm and weighting it with the spectrum of a 300 K blackbody. The uncertainty for the IR emittance measured with the portable equipment is ± 0.05 (confidence factor = 2).

Optical microscopy was performed using a Keyence VR-5000 microscope. Atomic Force Microscopy (AFM) was performed using a Bruker Dimension XR scanning probe microscope.

3. Results and Discussion

3.1 Conductive PEEK properties validation and space environment effect

In order to validate the use of material for space application, the assessment of their outgassing properties is needed especially for organic based material like thermoplastics. In the Table 1 here after the values of the total mass loss (TML), recovered mass loss (RML) and collected volatile condensable material (CVCM) values are presented. To be compliant to the ECSS-Q-ST-70-02C space standard material shall exhibit values of TML < 1 %, CVCM < 0.1 % and RML < 1 % [8]. For both PEEK and Conductive PEEK the outgassing properties meet this requirement and thus are eligible to be use as material in space. It is evident that the modification of a PEEK matrix using carbon-based fillers do not have significant effect on the outgassing properties.

Table 1: Outgassing properties of PEEK and conductive PEEK

Material	TML (%)	CVCM (%)	RML (%)
PEEK	0.30	0.00	0.15
Conductive PEEK	0.31	0.00	0.14

The processing capability of the conductive using the FFF process has been benchmarked using several 3D printers. In all cases, 3D printing parameters common to all 3D printers were fixed as followed: the extrusion temperature was set to 400 °C, the printing speed to 20 mm/s and the raster layer orientation or infill was +45°/-45°. Other parameters like print bed temperature, chamber temperature that depends on the intrinsic capability of each printers were optimised to the optimum capabilities of the used printers. It is important to mention that PEEK is one of the most difficult material to process via FFF. Due to its semi crystalline nature and high melting point (343 °C), the control of the thermal environment during the printing process is of paramount importance to enable optimised and controlled crystallisation kinetics and interlayer molecular diffusion to get good interlayer adhesion. The effect of the 3D printing process on the mechanical performance of PEEK based parts and the induced anisotropy is well known [10]. Since the commercialisation of the first printers in the early 2015 capable to process PEEK this issue has been minimised due to the progress in the development of 3D printers that have more and more accurate capability to control the thermal environment during printing. As it can be seen in Table 2, conductive PEEK has been processed using 3 different commercially available 3D printers with different market release time. The resulting flexural properties exhibit an increase by a factor 1.8 for the flexural modulus and 1.3 for the flexural strength when using a printer release on the market in 2021 compare to the one from 2018.

Table 2: Flexural properties of conductive PEEK processed as function of the 3D printer used

Printer Type	Flexural modulus (Gpa)	Flexural strength (Mpa)	Flexural strength @ 3.5% deformation (Mpa)	Failure
Printer 2018	2.48	117	92	interlayer
Printer 2020	4.40	142	125	no
Printer 2021	4.65	156	131	no

The effect of the UV/VUV exposure on 3D printed PEEK sample is illustrate in Figure 4. Optical microscopic imaging detect a slight discoloration. The UV/VUV exposure is the main cause of the change observed in the optical properties. This effect is confirmed by the thermo-optical measurements performed on the expose surface of the 3D printed sample in Table 3. After the combine UV/VUV exposure and Thermal vacuum cycling (TVAC), the thermal emittance did not significantly changed whereas the solar absorptance coefficient is decrease from 0.94 to 0.91.
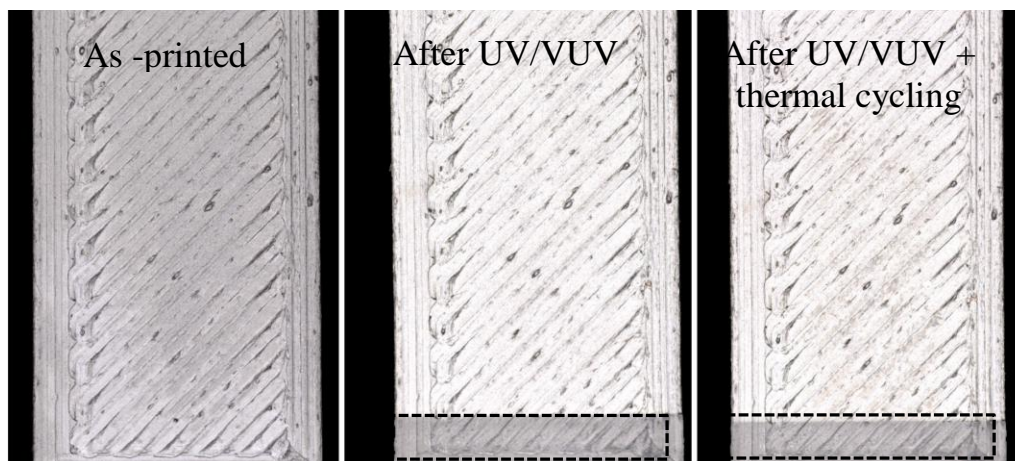

Figure 4: Optical image of conductive PEEK sample as-printed (Left), after UV/VUV exposure (Middle) and after UV/VUV exposure and thermal cycling (Right). The dashed area indicates an UV/VUV masked area during test.

Table 3: Measured solar absorptance and thermal emittance coefficient from the surface of 3D printed conductive PEEK samples subjected to different environmental exposure

Exposure type	Solar Absorptance (α)	Thermal Emittance (ε)
As-printed	0.94	0.87
After VUV+TVAC	0.91	0.86
After ATOX	0.97	0.93

The flexural properties of the samples exposed to different environment are presented in Table 4. Whereas being exposed to UV/VUV and TVAC or only TVAC, the flexural properties are not drastically affected. The main noticeable change is related to the flexural strength that is decreased by 5% after UV/VUV and thermal cycling exposure.

Table 4: Effect of environmental exposure on the flexural properties of 3D printed conductive PEEK samples

Samples conditioning	Flexural Modulus (GPa)	Flexural strength (MPa)
As-printed	2.48	117
After UV/VUV+TVAC (6 cycles)	2.47	111
After TVAC (20 cycles)	2.41	118

The effect of atomic oxygen (ATOX) on the surface of 3D printed conductive PEEK samples has been evaluated on two type of samples with different exposed surface state: one with a unmodified surface (as printed) and one with a surface that has been grinded using 400 grit sand paper. The received ATOX fluence during the exposure depends of the sample location in the chamber. For the as-printed sample, the fluence was 1.07×10^{21} atoms/cm^2 and for the grinded sample 2.12×10^{21} atoms/cm^2. Using a density of 1.31 g/cm^3 the calculated erosion yield were 2.35×10^{24} and 1.98×10^{24} cm^3/atom for the as-printed and grinded sample, respectively. Compare to exposure to UV/VUV, ATOX exposure leads to an increase in both solar absorptance and thermal emittance coefficient (Table 3). Thermal emittance coefficient that was 0.87 for the as printed sample is increase to 0.93 after exposure to ATOX. The solar absorptance is increase from 0.94 to 0.97. This effect on the change of the thermo-optical properties is to be related to the change of surface state. The difference of surface state for the as-printed sample before and after ATOX exposure is presented in Figure 5. A clear erosion phenomenon is occurring leading to change in the surface texture and morphology.
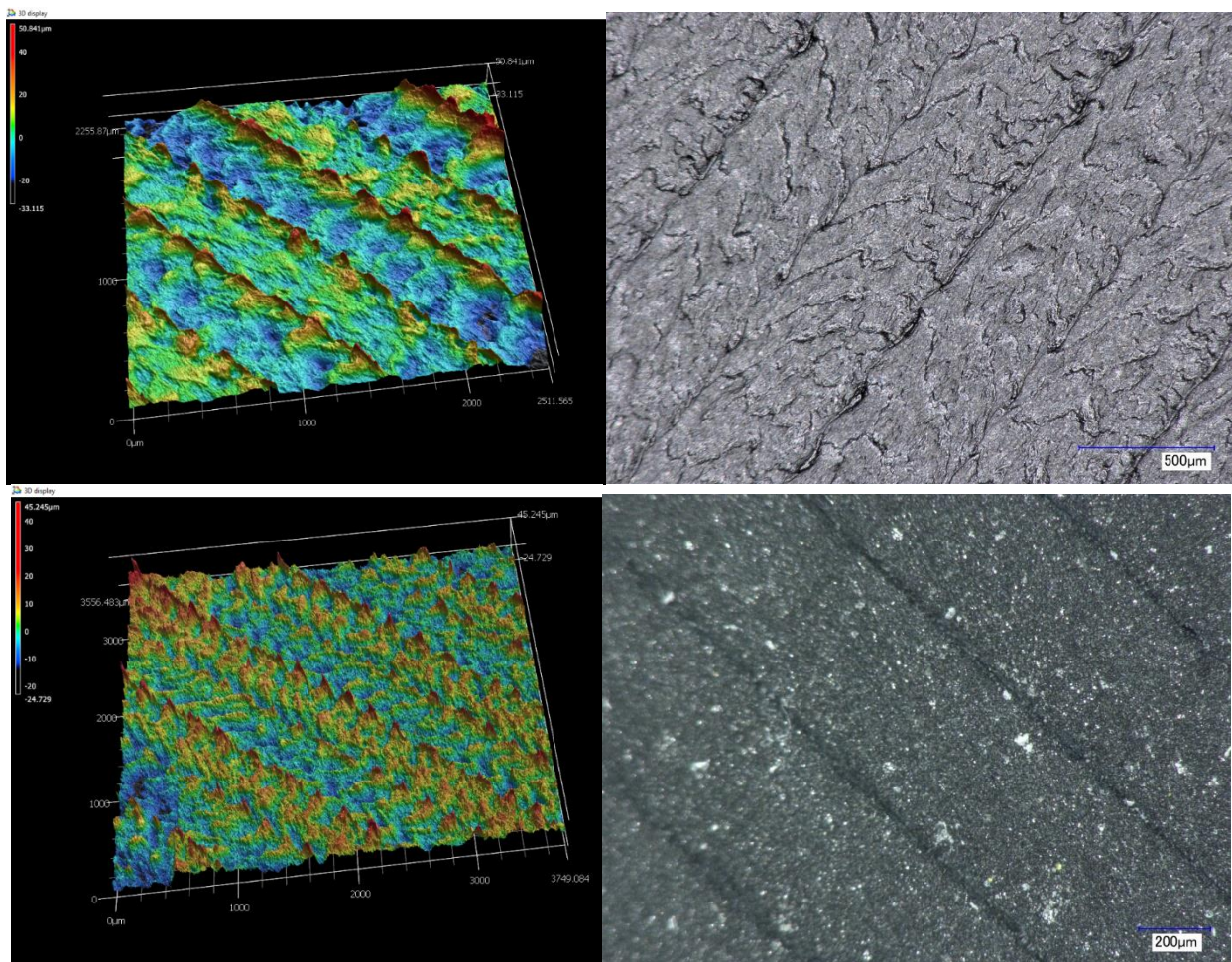

Figure 5: Surface morphology of the non-exposed (Top) and ATOX exposed (Bottom) area.

The change in the surface morphology has been further investigated by AFM on several 10 x 10 μm area. The pictures presented in Figure 6 shows two different imaging mode obtained either using adhesion mapping or height mapping. The evolution of the surface roughness presented in Table 5 has been calculated using the Bruker NanoScope software suite on several location for both expose and non-exposed areas. The pitting effect generated by the highly reactive atomic oxygen species leads to huge increase of the surface roughness. In average, all roughness related parameters (Rq, Ra and Rmax) are increased, by a factor 10.

Table 5: Variation of the roughness parameters before and after ATOX exposure

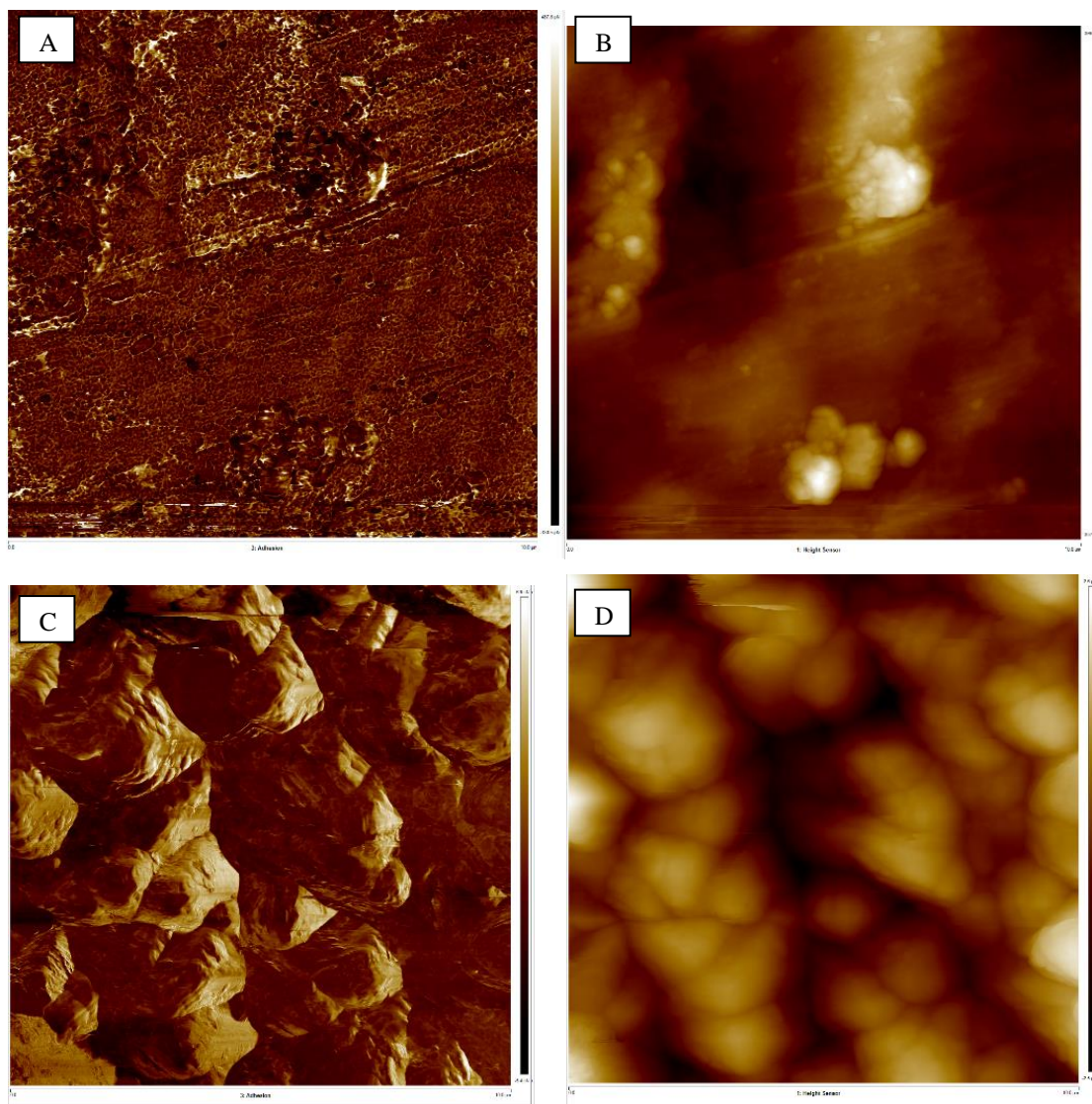| Sample (10 x 10 μm)	RMS Roughness Rq (nm)	Roughness Average Ra (nm)	Max Roughness Depth Rmax (nm)
Non Exposed	94-115	70-92	641-791
ATOX Exposed	733-1380	583 -1100	4780 - 10276

Figure 6: Surface morphology using AFM adhesion mode (A,C) and height mode (B,D) for a non-exposed area (A and B) and ATOX exposed area (C and D)

To complete the assessment of the suitability of the conductive PEEK for space application, its behaviour toward electrical charging was investigated in vacuum condition ($<10^{-6}$ mbar) at room temperature (300 K) and at cryogenic condition (93 K). For this purpose, using the dedicated ESD facility, the sample surface was irradiated with 5 keV electron for 5 min. After irradiation, the evolution of surface potential was monitored as function of time. This evolution is plotted in Figure 7. It can be seen that at 300 K, the charges accumulated during irradiation are directly evacuated from the surface sample (the potential return to a 0 V state). At cryogenic condition, the kinetic associated to the discharge capability is increased: it takes 0.9 h for the potential to recover a 0 V state. Effect of temperature of charge mobility along the sample surface is expected. In both case, the electrical conductive PEEK is capable to drain accumulated surface electrons through its bulk enabling this material to be ESD safe and thus compliant for its use in space environment.
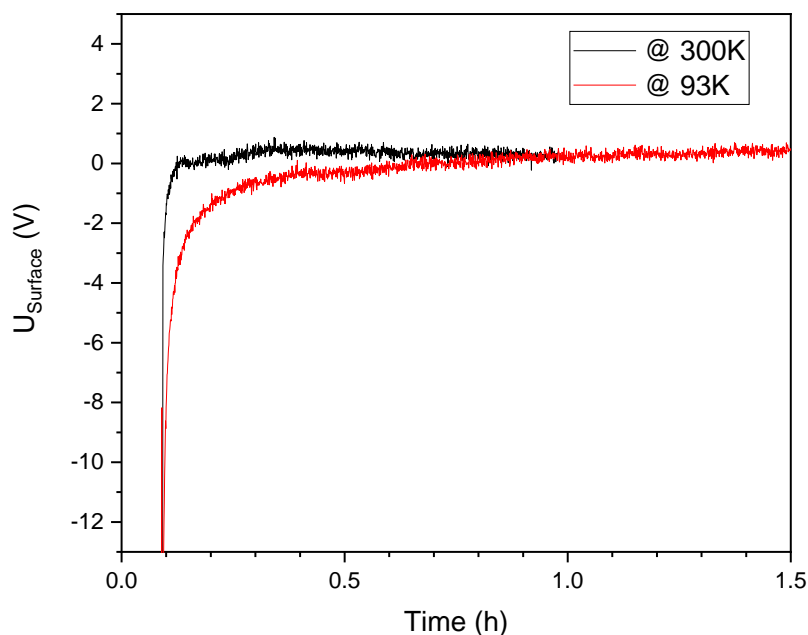

Figure 7: Evolution of the surface potential of a 3D printed conductive PEEK sample at 300 and 93 K

From this test campaign, the main goal was to assess the capability of 3D printed parts made of electrically conductive PEEK to perform under space environment. From past and on-going studies, this material is fully suitable to be process using the FFF process (3D printing). It has been demonstrated that the mechanical performance of this material are not affected by thermal cycling or UV/VUV exposure corresponding to 3.4 solar constant. However, atomic oxygen exposure leads to erosion and pitting resulting in a surface roughness change and an evolution of the thermos-optical properties. However, the erosion yield are below the one reported for PEEK ($\sim 3.03 \times 10^{24}$ cm^3/atom) gathered from the MISSE 2 PEACE experiment during real space exposure [11]. Due to its intrinsic electrical conductivity, parts made of electrically conductive PEEK are capable to generate enough charge mobility even at cryogenic temperature to avoid ESD phenomenon.

3.2 PEEK – Conductive PEEK prototype manufacturing and testing

Taking advantage of the suitability of this material from a space environment perspective, this will enable new application. For example, metal part replacement is under investigation in other ESA led studies taking advantage of the use of 3D printing and focussing on the mass reduction of structural parts compare to a metallic based counterpart [1], [3]. Another elegant way to take advantage of this material is the manufacturing of electrical circuit. Using PEEK and conductive PEEK together with a 3D printing process, embedded conductive path can be created within a part. However, before designing such concept, it is important to understand if bi-material printing process can be achieved using two different blends of PEEK and how the interface will behave. In order to do so, the flexural performance of sample produced using bi-material printing capability with PEEK and conductive PEEK has been assessed. The results presented in Figure 8 show that the PEEK/conductive PEEK interface are stable and do not create a weak interface. The flexural modulus obtained for the bi-material sample lies between the flexural modulus of the PEEK and conductive PEEK. The flexural strength of the sample made from PEEK and conductive PEEK present a similar

behaviour with a strength at yield of 146 and 142 MPa, respectively. The composite samples made out two different PEEK materials exhibits a slight decrease of flexural strength as seen in Figure 8 with a strength at yield of 133 MPa. However, for all configuration tested, no interlayer delamination has been observed with the bulk or at the PEEK/Conductive PEEK interface. A demonstrator made of PEEK with embedded conductive PEEK line and metallic connectors was subjected to thermal vacuum cycling in a previous study. Both electrical measurement and CT Scan investigation did not detect any effect of the thermal vacuum cycling on the electrical conduction capability or interface degradation between the two different blend of PEEK [7].
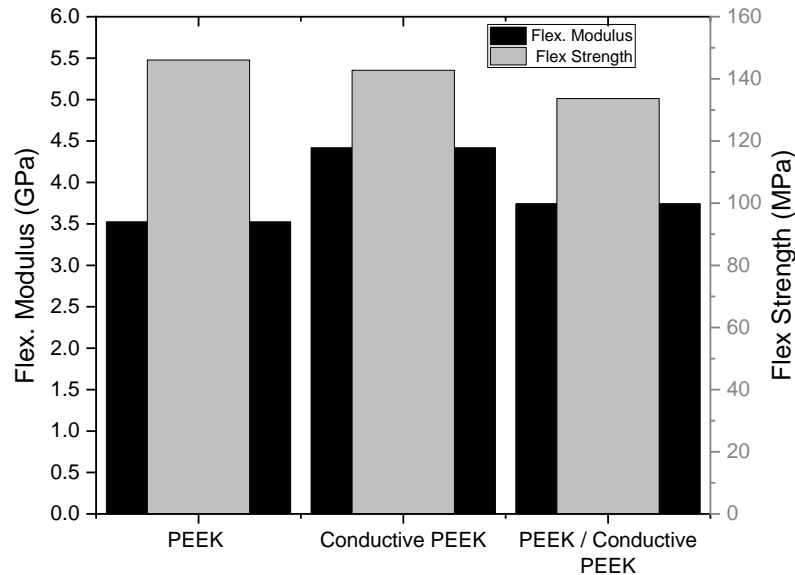
Figure 8: Flexural modulus (Right – Black) and strength at yield (Left – grey) for PEEK, conductive PEEK and bi-material PEEK/conductive PEEK sample

These results give confidence in the capability of producing parts using bi-material printing capability using PEEK and conductive PEEK without any issues related to interface mismatch or manufacturability. It was decided to design a prototype to be implemented on a future CubeSat mission (WISA WoodSat [12]) as a payload to test the potential of this material and process combination for electrical circuit application (Figure 9 and 10).
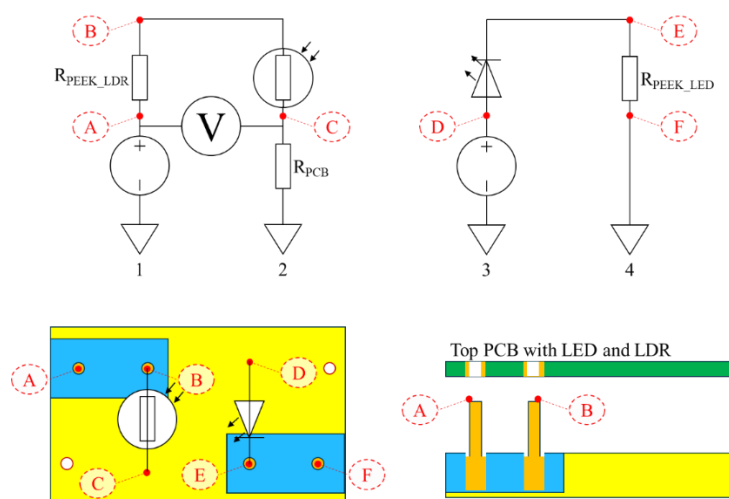

Figure 9: Schematic of the 3D printed demonstrator equivalent electrical circuit diagram for (Top left) the light sensing part and (Top right) the light emitting part. (Bottom) top and side view (PEEK in yellow, conductive PEEK in blue and gold platted metallic pins orange). The red dashed elliptic flags identified by a letter pinpoint positions in the equivalent circuit diagram and their corresponding positions on the schematics.
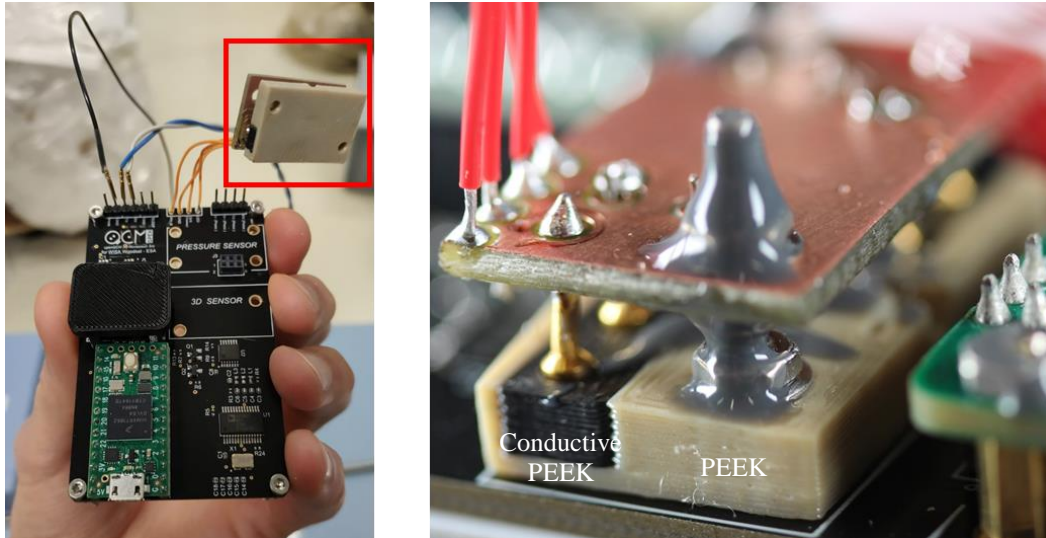
Figure 10: (Left) Picture of 3D printed demonstrators for CubeSat (red rectangle) during integration. (Right) demonstrator fixed to the main PCB with the visible 3D printed conductive PEEK path (black), the PEEK main body (beige) and the top PCB sandwiching against the PEEK a LED and a LDR (not visible on the picture).

In order to assess the functionality of the 3D demonstrator for CubeSat in vacuum and temperature representative conditions, an QM payload has been tested in the BOF facility at a pressure below 10-6 mbar and between +60 and -20 C. The aim of this test is to demonstrate functionality of the 3D printed demonstrator in vacuum at representative mission temperature. For this purpose, at regular intervals, the LED was turned on for a second and during the entire duration of the test, the amplitude of the voltage measured in the light sensing part (LDR) connected to the 3D printed demonstrator was monitored and recorded. Results are shown in Figure 11 and Figure 12. This test was done with a non-optimal measurement setting that induced noise and some loss of data transmission from the vacuum chamber to the multiplexer.
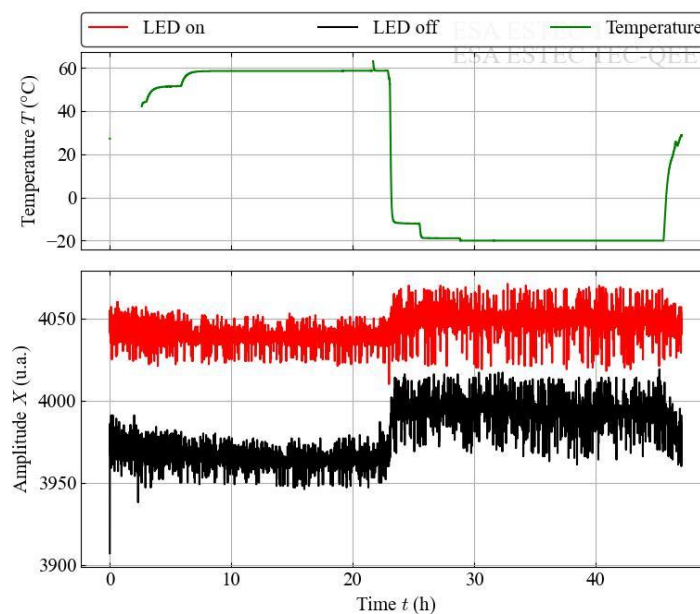

Figure 11: Evolution of the voltage amplitude of the LDR corresponding to difference of electric potential between flag A and C in Figure 9 as function of time and temperature.
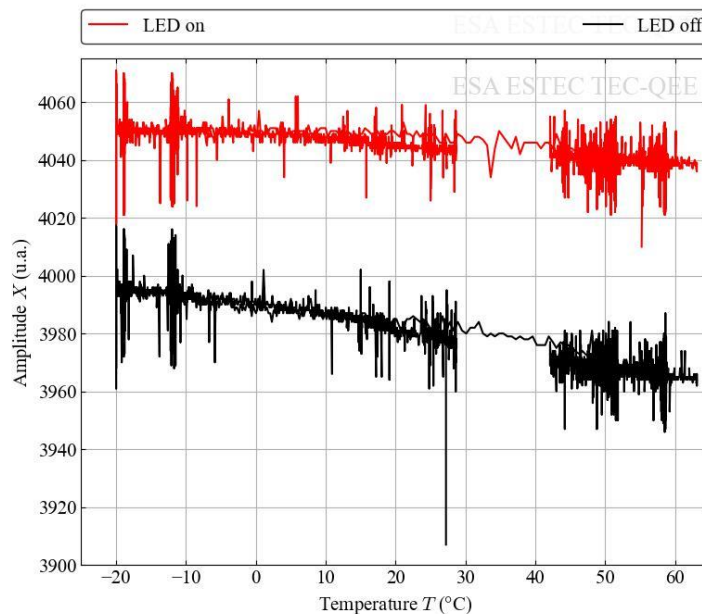
Figure 12: Evolution of the voltage amplitude of the LDR corresponding to difference of electric potential between flag A and C in Figure 9 as function of the mission representative temperature

The 3D printed demonstrator for CubeSat and its measurement chain on the ESA payload main PCB was functional in vacuum in mission representative temperatures. The difference of amplitude that can be measured between LED on and LED off state is sufficient to allow optical transfer of information in-orbit. This set-up will be use in orbit to demonstrate optical transfer of information using 3D printed condutcive PEEK as an electrical conductor. The continuous monotoring of the evolution of the amplitude value will also be useful to evaluate the in-orbit ageing of the materials.

4. Conclusion

Development of electrically conductive thermoplastics suitable for space environment was demonstrated in this study. The combination of such multifunctional material with FFF process (3D printing) is well suited for part production for space application. The proposed demonstrator is one of many potential example that could be enable by using material with enhanced properties together with 3D printing. The development of this CubeSat payload has been achieved in very short time frame due to the versatility of the material/process combination. Looking into the future, besides using this material to replace metallic parts produced on ground, this material will be very suitable as feedstock for out-of-earth or in-space manufacturing capabilities. Indeed, using thermoplastics will ease recycling and in addition, the FFF process has been demonstrated to work perfectly in microgravity and under vacuum condition [13]. Material with enhanced and demonstrated capability will enable new mission scenario and specially for maintenance purpose and on demand manufacturing whereas on ground or out-of-earth [14].

Acknowledgement

References

[1]   "HighPEEK | ESA TIA." [Online]. Available: https://artes.esa.int/projects/highpeek.
[2]   "Destination - 3D Printed satellite parts." [Online]. Available:
        https://minifactory.fi/blog/destination-3d-printed-satellite-parts/.

[3]   L. Nyman *et al.*, "Overview of ground-based testing of components made from electrically-conducting doped PEEK for space applications," in *Proceedings of the 20th European Conference on Composite Materials*, 2022.

[4]   J. Gonçalves *et al.*, "Electrically Conductive Polyetheretherketone Nanocomposite Filaments: From Production to Fused Deposition Modeling," *Polymers (Basel).*, vol. 10, no. 8, p. 925, Aug. 2018.

[5]   "ESA - 3D printing CubeSat bodies for cheaper, faster missions." [Online]. Available: https://www.esa.int/Enabling_Support/Space_Engineering_Technology/3D_printing_CubeSat_bodies_for_cheaper_faster_missions.

[6]   "ESA - Portrait transmitted via 3D printing." [Online]. Available: https://www.esa.int/ESA_Multimedia/Images/2020/11/Portrait_transmitted_via_3D_printing.

[7]   J. Krywko, U. Lafont, M. Siemaszko, D. Piastowski, W. Namiotko, and D. Dudenko, "3D Printing CubeSat Parts with Power and Data Transfer Functionalities with Two Blends of PEEK," in *2022 IEEE Aerospace Conference*, 2022.

[8]   European Cooperation For Space Standardization, "ECSS-Q-ST-70-02C: Thermal vacuum outgassing test for the screening of space materials," 2008.

[9]   B. Delacourt *et al.*, "Materials charging investigations for JUICE," *CEAS Sp. J.*, vol. 13, no. 3, pp. 493–508, Jul. 2021.

[10]   A. R. Zanjanijam, I. Major, J. G. Lyons, U. Lafont, and D. M. Devine, "Fused filament fabrication of peek: A review of process-structure-property relationships," *Polymers (Basel).*, vol. 12, no. 8, p. 1665, Aug. 2020.

[11]   B. A. Banks, J. A. Backus, M. V Manno, D. L. Waters, K. C. Cameron, and K. K. De Groh, "Atomic oxygen erosion yield prediction for spacecraft polymers in low earth orbit," *ntrs.nasa.gov*, 2009.

[12]   "ESA - ESA flying payloads on wooden satellite." [Online]. Available: https://www.esa.int/Enabling_Support/Space_Engineering_Technology/ESA_flying_payloads_on_wooden_satellite.

[13]   M. Quinn, U. Lafont, J. Versteegh, and J. Guo, "Effect of low vacuum environment on the fused filament fabrication process," *CEAS Sp. J.*, vol. 13, no. 3, pp. 369–376, 2021.

[14]   A. Makaya, L. Pambaguian, T. Ghidini, T. Rohr, U. Lafont, and A. Meurisse, "Towards out of earth manufacturing: overview of the ESA materials and processes activities on manufacturing in space," *CEAS Sp. J.*, vol. 1, pp. 1–7, Mar. 2022.